# Separation of Mineral Acid Solutions by Membrane Distillation and Thermopervaporation through Porous and Nonporous Membranes

**DATASET** *in* INDUSTRIAL & ENGINEERING CHEMISTRY RESEARCH · JULY 2013

Impact Factor: 2.59 · DOI: 10.1021/ie3025246



**4 AUTHORS**, INCLUDING:

Valery. Vycheslavovich. Ugrozov
Finance University under the Government of t…
**42** PUBLICATIONS **117** CITATIONS
SEE PROFILE

Vladimir V. Volkov
Institute of Petrochemical Synthesis
**88** PUBLICATIONS **979** CITATIONS
SEE PROFILE

I&EC research
Industrial & Engineering Chemistry Research

Article

pubs.acs.org/IECR

# Separation of Mineral Acid Solutions by Membrane Distillation and Thermopervaporation through Porous and Nonporous Membranes

Inga B. Elkina,[†] Alla B. Gilman,[‡] Valery V. Ugrozov,[§] and Vladimir V. Volkov*[,†]

[†]Topchiev Institute of Petrochemical Synthesis, RAS, Leninsky pr.29, 119991 Moscow, Russia

[‡]N.S. Enikolopov Institute of Synthetic Polymer Materials, RAS, Profsoyuznaya st.70, 117393 Moscow, Russia

[§]The All Russian Institute of Finance and Economic, Moscow, Russia, Oleko Dundich str., 123995, Moscow, Russia

**ABSTRACT:** Membrane distillation was suggested for the regeneration of volatile inorganic acids (hydrochloric and nitric acids) from the metal pickling solutions using hydrophobic porous and nonporous asymmetric membranes. The investigations were performed with a flat-sheet commercial microfiltration membrane based on tetrafluoroethylene/vinylidenefluoride copolymer MFF-2 and with a plasma-modified commercial asymmetric gas separation membrane based on poly(vinyltrimethyl silane) (PVTMS). The influence of acid concentration (varying over a wide concentration range from 0.01 to 7.0 N) and the feed temperature ($T_h$ = 313−333 K) on the transmembrane flux and selectivity was studied. It was shown that the concentrating of volatile inorganic acids in the feed using a porous MFF-2 membrane is effective up to 1.0 N concentration. Plasma-modified PVTMS membrane was used for the separation of feed solutions with higher acid content up to 7.0 N. It was established that the plasma treatment essentially increases the hydrophilic properties of PVTMS membrane surface.

## 1. INTRODUCTION

Membrane distillation (MD) is a nonisothermal process which involves evaporation of volatile compounds through a porous hydrophobic membrane. Therefore, in the MD process, the mechanism of separation is based on the vapor/liquid equilibrium of the liquid mixture. The benefits of the MD process involve lower operating temperatures (as compared with conventional distillation), lower hydrostatic pressures (as compared with membrane pressure-driven processes, for example, reverse osmosis), the high rejection factor for nonvolatile solutes (salts, colloids, etc.) as well as the possible use of waste heat and renewable energy sources. Hence, this potential makes this MD approach more advantageous over many other popular separation processes.[1]

Depending on the modes of driving force generation and permeate collection, various types of MDs are known: a direct-contact MD (DCMD), an air gap MD (AGMD), a sweeping gas MD (SGMD), and a vacuum MD (VMD). In the DCMD, both the liquid feed and liquid permeate are kept in contact with the membrane, and the temperature difference between the two solutions gives rise to a transmembrane vapor pressure difference that drives the flux. The mass transfer is accompanied by the transfer of the corresponding latent heat plus the conductive heat leak through the membrane. It is worth mentioning that the DCMD is the most studied MD configuration even though the heat transferred by conduction through the membrane is higher than that in the other MD configurations. More than 60% of the MD studies are focused on the DCMD systems.[1] The DCMD appears to be the best choice for the applications when a major permeating component is water, for example, desalination or concentration of aqueous solutions.[3−11] Deaerated DCMD systems were also investigated in order to improve mass transfer within the membrane pores.[12−14]

The basic limitation of the MD approach is related with the fact that the process solutions should be aqueous solutions and they should be sufficiently diluted to prevent any wetting of the hydrophobic porous membrane. This factor limits the potential of the MD approach in such applications as desalination for pure water production[2] and concentration of some nonvolatile solutes in aqueous solutions (salts, fruit juices, etc.).[15−17] Moreover, the MD approach can be used for the separation of volatile solutes in aqueous mixtures. For example, this concerns separation of water−organic mixtures[18−20] and inorganic acids aqueous solutions.[21−24] Dehydration of nitric acid by vacuum pervaporation on a specially made Nafion composite ionomer membrane was also studied.[25,26]

The objective of the present study is to investigate the separation of nitric acid and hydrochloric acid aqueous solutions over a wide range of concentrations using porous and nonporous polymeric membranes by DCMD and thermopervaporation (TPV), respectively. Noteworthy is that the TPV method (first proposed by Aptel[27] in 1976) is still less investigated mode of pervaporation separation. This process is similar to the MD method but a nonporous membrane is used. Recently, the TPV process has attracted a keen interest as an effective energy-saving approach for the removal of bioethanol[27] and biobutanol[29,30] from the fermentation broths. In the case of MD, a microfiltration hydrophobic membrane based on tetrafluoroethylene−(vinylidene fluoride) copolymer was used. For the TPV of inorganic acids, a gas-separation hydrophobic asymmetric membrane based on poly(vinyltrimethylsilane)

**Special Issue:** Giulio Sarti Festschrift

**Received:** October 1, 2012
**Revised:** February 14, 2013
**Accepted:** February 15, 2013
**Published:** February 15, 2013





dx.doi.org/10.1021/ie3025246 | *Ind. Eng. Chem. Res.* 2013, 52, 8856−8863

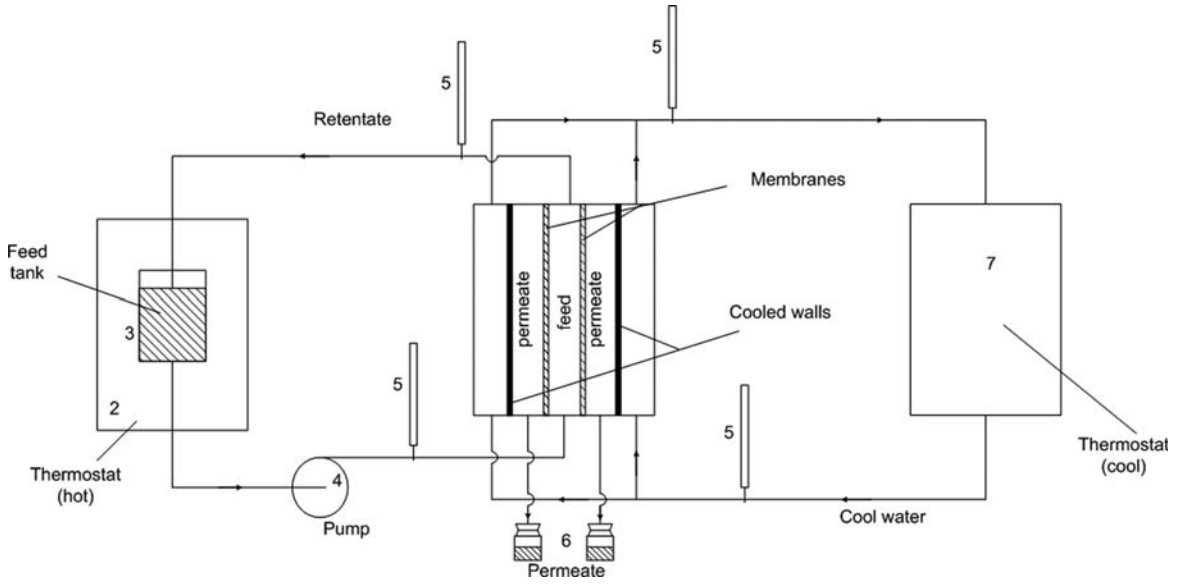


**Figure 1.** Schematic representation of the labscale setup for the thermogradient separation method.

(PVTMS) was employed. To improve both transport and selective properties, the PVTMS membrane was modified in a low-frequency glow discharge (50 Hz) in air.

## 2. EXPERIMENTAL SECTION

**2.1. Membrane.** The MD process was studied with a flat-sheet commercial microfiltration membrane of the type MFF-2 made from a copolymer of tetrafluoroethylene and vinylidene fluoride (ZAO NTC "VLADIPOR", Vladimir, Russia). The average pore size was 0.25 $\mu$m, the overall thickness was 120 $\mu$m, and the porosity was about 70%.

For the TPV separation experiments we used a commercial poly(vinyltrimethylsilane) (PVTMS) gas separation membrane (PC-375-C-2.5 brand). The membrane is asymmetric and consists of two layers: a selective membrane skin 0.2 $\mu$m thick, which is responsible for the membrane selectivity and flux, and a porous support 120 $\mu$m thick.[31]

**2.2. Experimental Separation Setup.** The experimental study of DCMD and TPV processes for volatile inorganic acid solutions was carried out on a labscale setup (Figure 1). This setup involves the following units: a flat-plate module (1); a thermostat (2) equipped with a special vessel (3) where the feed solution is heated to the desired temperature; a pump (4); thermometers (5) for controlling the input and output temperatures; graduated cylinders (6) for collecting permeate and, finally, a circuit of cooling water (7). The flat-plate MD-module contains three types of chambers: two chambers for the circulation of cooling water, two chambers for permeate collection, and a central chamber for the circulation of the feed solution. Two different membranes can be tested simultaneously in one experimental run.

The experiments were carried out under the following conditions: The temperature of the heated feed solution was 313−333 K, the temperature of the cooling water was 293 K, the flow rates of the feed solution and the cooling water were 40 L/h and remained constant in all the experiments. The acid concentrations in the feed solutions and permeate were determined by titration using a BAT-15 automatic installation (accuracy, $\pm 1 \times 10^{-4}$ g/L). The permeate quality was controlled by measuring its conductivity, which was determined with a KEL-1 M conductometer with platinum reference electrodes calibrated with respect to KCl standard solutions.

**2.3. Plasma Modification Method.** The PVTMS membrane was modified in a low-frequency glow discharge using a vacuum plasmochemical setup (Figure 2) according to

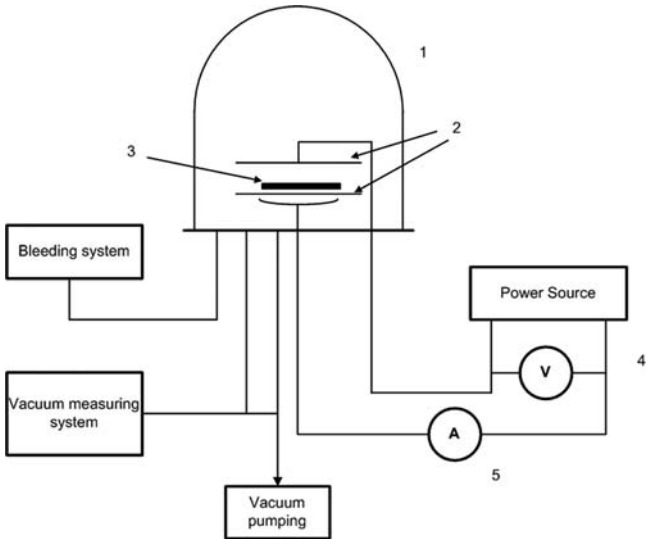


**Figure 2.** Scheme of the laboratory plasma setup: (1) bell jar, (2) electrodes, (3) membrane sample, (4) voltmeter, (5) ampermeter.

ref 32. Electrodes ($210 \times 120$ mm$^2$) were placed horizontally in the reaction chamber at a distance of 50 mm one from another. The PVTMS membrane ($40 \times 100$ mm$^2$) was put on the center of the lower electrode, its selective membrane skin being directed to the discharge zone. Air was used as the plasma-forming gas.

**2.4. Contact Angle Measurements.** Variation in the membrane surface properties was studied by measuring the contact angle ($\theta$) by a goniometric method using an Easy Drop DS100 (KRUSS, Germany), and images were acquired using a Drop Shape Analysis V.1.90.0.14 software. Deionized water and glycerol were used as the working liquids.[32] On the basis of the experimental values of $\theta$, the work of adhesion ($W_a$), total


dx.doi.org/10.1021/ie3025246 | Ind. Eng. Chem. Res. 2013, 52, 8856−8863

surface energy ($\gamma$), and its polar ($\gamma^p$) and dispersion ($\gamma^d$) components were calculated according to the Young equation.[33] For the initial membrane, the $\theta$ values were found to be 109° (by water) and 98° (by glycerol). Hence, this evidence proves that the membrane surface is hydrophobic.

**2.5. IR-Spectroscopy.** The IR spectra of the PVTMS membrane were collected on a Biorad FTS-60 spectrometer equipped with an ATR attachment (resolution, 2 $cm^{-1}$). A KRS-5 crystal with an incident beam angle of 45° and 25-fold reflection was used as the internal reflection element.

**2.6. Surface Potential Measurements.** Surface potential of the membranes was measured by the dynamic capacitance technique.[34] The measurements of dielectric permeability ($\varepsilon$) for the initial and modified samples show that $\varepsilon$ is constant at any discharge parameters. This fact allowed us to estimate the surface charge density (accuracy, ± 5%) from the surface potential data.[35]

The charge-transfer processes in membranes were studied by the thermostimulated relaxation (TSR) and thermostimulated depolarization (TSD) methods and by measuring the membrane conductivity in the temperature interval from 300 to 430 K (accuracy, ± 5%).[34] The TSR of these samples was measured immediately after the plasma treatment at a heating rate of 2 K/min. PVTMS is known to have two high-temperature relaxation transitions near 393 and 443 K, the lower temperature is associated with the glass transition temperature $T_g$; the melting point is 513 K.[36−38] Therefore, in the TSD measurements, a membrane was first heated to 400 K and then was polarized in a field with a voltage of 1000 V/mm at 430 K for 15 min. Then, the membrane was cooled down to the room temperature at a cooling rate of 2 K/min, and the external field was switched off. The TSD measurements were carried out under the conditions of linear heating at a rate of 2 K/min.[39]

## 3. RESULTS AND DISCUSSION

**3.1. Membrane Distillation Using Porous MFF-2 Membrane.** The peculiarity of separation of inorganic acid aqueous solutions is that the vapors of two volatile components (water and acid) are transferred through the membrane pores. We studied experimentally the effect of acid concentration in the feed solution (for nitric acid, from 0.05 to 4.6 N; for hydrochloric acid, from 0.001 to 5.4 N) on the transmembrane flux and on the retention coefficient at various temperatures of the feed solution supplied to the module ($T_h$ = 313, 323, and 333 K).

The transmembrane flux reads as

$$J = \frac{m}{St} \tag{1}$$

The retention coefficient was estimated according to:[40]

$$R_i = 1 - \frac{C_{i,p}}{C_{i,f}} \tag{2}$$

Figures 3 and 4 present the experimental fluxes and retention coefficients plotted against acid concentration in the feed solution at three different temperatures. As the acid concentration increases, the efficacy of the MD process markedly decreases. For example, for hydrochloric acid solutions (Figure 3), the flux of the 5.4 N solution decreases by a factor of approximately 2.9, 2.7, and 2.2 as compared with the flux for the starting 0.001 N HCl solution at 313, 323, and 333 K, respectively. Similar dependences are observed for the $J$ values in the case of nitric acid solutions (Figure 4). Hence, the flux for the 4.6 N $HNO_3$ solution is 3.4, 2.3, and this value is 1.8 times lower than that for the starting 0.05 N solution at 313, 323, and 333 K, respectively. Nevertheless, the flux values are, on average, 8−20 kg/($m^2$h) within the studied temperature interval of the feed solution (313−333 K) and for the temperature gradient across the membrane $\Delta T$ = 20−40 K. This is quite suitable for practical use.

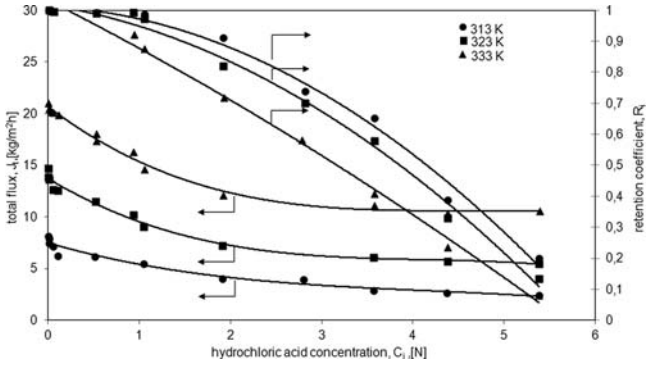


**Figure 3.** Total flux and retention coefficient plotted against hydrochloric acid concentration in the feed solution at temperatures $T_h$ = 313, 323, and 333 K.

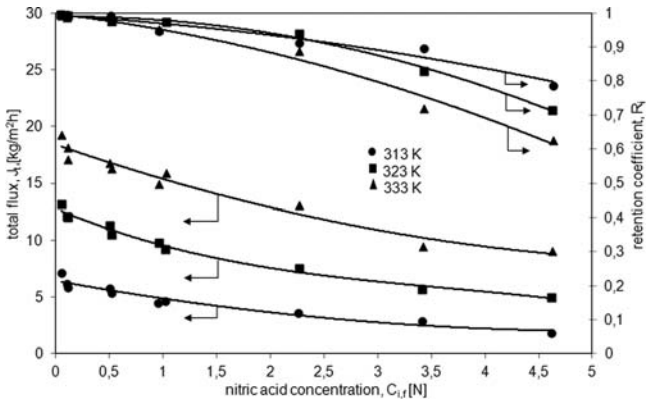


**Figure 4.** Total flux and retention coefficient plotted against nitric acid concentration in the feed solution at temperatures $T_h$ = 313, 323, and 333 K.

For the solutions of hydrochloric acid (Figure 3), the retention coefficient for the 5.4 N solution decreases by a factor of approximately 5, 7.5, and 12.5 as compared with that of the starting 0.001 N HCl solution at 313, 323, and 333 K, respectively. In the case of the nitric acid solutions, a slower decrease in the retention coefficient ($R_j$) (relative to hydrochloric acid) is observed. Thus, for the 4.6 N $HNO_3$ solution, $R_j$ decreases, on average, by a factor of 1.4 as compared with that for the 0.05 N starting solution. This difference is associated with the different behavior of the saturated vapors of water and acids depending on temperature and concentration of acid solutions.[41]

In the MD process, the feed and permeate compositions are presented in Tables 1 and 2 for hydrochloric and nitric acids, respectively. In the initial region of feed composition, the permeate is seen to contain minor acid quantities. The acid content starts to appreciably increase at the feed concentration interval above ~1 N and 2 N for HCl and $HNO_3$, respectively. This behavior of the permeate composition agrees qualitatively


dx.doi.org/10.1021/ie3025246 | Ind. Eng. Chem. Res. 2013, 52, 8856−8863

**Table 1. Concentration of Hydrochloric Acid in the Feed and Permeate at Different Temperatures of the MD Process**

| | $C_{i,p}$ [N] | | |
|---|---|---|---|
| | $T_h$ = 313 K | $T_h$ = 323 K | $T_h$ = 333 K |
| $C_{i,f}$ [N] | $T_c$ = 293 K | $T_c$ = 293 K | $T_c$ = 293 K |
| 0.001 | 0.000004 | 0.000003 | 0.000005 |
| 0.005 | 0.00002 | 0.00002 | 0.00003 |
| 0.01 | 0.00007 | 0.00006 | 0.00008 |
| 0.05 | 0.0004 | 0.0003 | 0.00045 |
| 0.10 | 0.0009 | 0.0009 | 0.001 |
| 0.50 | 0.0055 | 0.0055 | 0.009 |
| 0.91 | 0.01 | 0.0109 | 0.0729 |
| 1.02 | 0.0153 | 0.0296 | 0.128 |
| 1.88 | 0.173 | 0.346 | 0.53 |
| 2.77 | 0.728 | 0.839 | 1.163 |
| 3.54 | 1.234 | 1.496 | 2.097 |
| 4.35 | 2.678 | 2.93 | 3.348 |
| 5.37 | 4.304 | 4.664 | 4.948 |

**Table 2. Concentration of Nitric Acid in the Feed and Permeate at Different Temperatures of MD Process**

| | $C_{i,p}$ [N] | | |
|---|---|---|---|
| | $T_h$ = 313 K | $T_h$ = 323 K | $T_h$ = 333 K |
| $C_{i,f}$ [N] | $T_c$ = 293 K | $T_c$ = 293 K | $T_c$ = 293 K |
| 0.05 | 0.0002 | 0.0002 | 0.0004 |
| 0.10 | 0.0005 | 0.0004 | 0.0010 |
| 0.50 | 0.0035 | 0.0100 | 0.0120 |
| 1.00 | 0.0230 | 0.0240 | 0.0270 |
| 1.93 | 0.0495 | 0.0458 | 0.0458 |
| 2.24 | 0.1990 | 0.1430 | 0.2505 |
| 3.40 | 0.3570 | 0.5810 | 0.9518 |
| 4.61 | 0.9870 | 1.3190 | 1.7155 |

with the liquid−vapor equilibrium curves for hydrochloric and nitric acids.

Therefore, vapors of volatile inorganic acids can be transferred through the porous MFF-2 membrane together with the water vapors. As a result, when the acid concentration in solution is, on average, above 2.0 N, the fraction of the volatile acid vapors is high and this value increases with increasing acid concentration and temperature of the feed solution. The same tendencies were observed for separation of HCl and $HNO_3$ aqueous solutions using DCMD through PTFE flat and PP capillary porous membranes.[22] As it was demonstrated in ref 42, this approach makes it possible to separate acids from nonvolatile admixtures in the technological acid solutions, for example, dissolved salts of nonferrous and heavy metals.

**3.2. Plasma Modification of PVTMS Membrane.** Figure 5 shows the contact angle plotted as the function of the plasma treatment duration ($\tau$) (at the constant current, 80 mA). Figure 6 presents the plot of $\theta$ versus current (I) (at the fixed treatment duration, 30 s). As the treatment duration and current increase, $\theta$ dramatically decreases; this sharp decrease is followed by a gradual reduction in $\theta$ and, finally, a plateau is attained. The minimum $\theta$ values are observed when the treatment duration is 30−60 s and the current is 80−100 mA. From the experimental values of $\theta$ with respect to water and glycerol, the work of adhesion, and the total surface energy and its polar and dispersion components are calculated (Figures 5 and 6). When the treatment duration is longer than 30 s

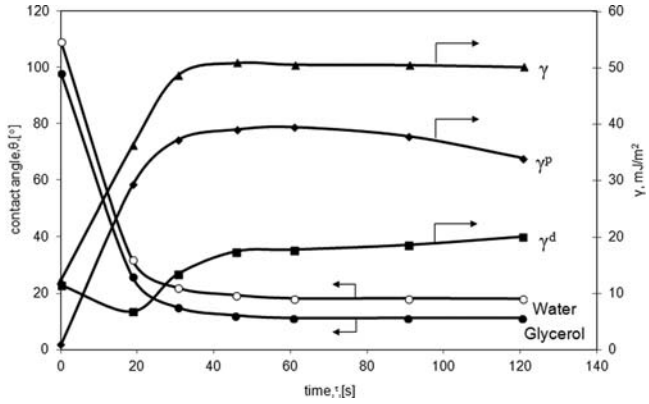


**Figure 5.** Contact angles for water and glycerol and surface energy of the modified PVTMS membrane plotted against the plasma treatment duration (50 Hz, $I$ = 80 mA).

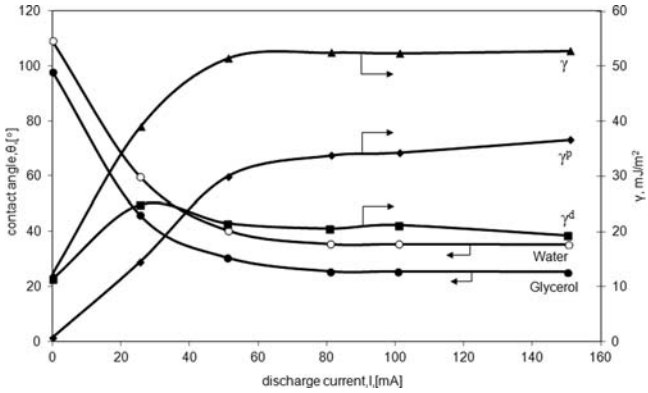


**Figure 6.** Contact angles for water and glycerol and surface energy of the modified PVTM membrane plotted against the discharge current (50 Hz, time = 30 s).

(Figure 5), the values of $\gamma$, $\gamma^d$, and $\gamma^p$ increase (relative to those of the initial PVTMS sample), on average, by a factor of 4.3, 1.5, or ∼40, respectively. At $I$ = 80 mA (Figure 6), $\gamma^p$ increases (by 40 times as compared with that of the initial sample), and the $\gamma$ and $\gamma^d$ values increase by a factor of 4.3 or 2.1, respectively. The experimental data indicate that the PVTMS-based membranes change their hydrophobic properties for hydrophilic.

From the standpoint of the practical membrane application, it seems crucial that the modified membranes should preserve their stable hydrophilic properties with time. Table 3 lists the $\theta$ values with respect to water and glycerol, $W_a$ (the work of adhesion), and $\gamma$, $\gamma^d$ ,and $\gamma^p$ for the set of the PVTMS-based samples after their plasma treatment under different conditions and storage for 46 days in air under standard conditions (room temperature, relative humidity). The $\theta$ values are seen to increase with time; however, in all cases, the PVTMS surface remains hydrophilic ($\theta$ < 60°). Comparison of the data presented in Figures 5 and 6 and in Table 3 makes it possible to conclude that the values of adhesion work and surface energy remain appreciably higher than those of the initial PVTMS, although they tend to decrease with time.

**3.3. IR-Spectroscopic Results.** The composition of functional groups on the selective skin surface of the plasma-modified PVTMS membranes was studied by the ATR spectroscopic technique. The absorption bands in the range 1500−1800 $cm^{-1}$ (which are characteristic of carbonyl- and


dx.doi.org/10.1021/ie3025246 | Ind. Eng. Chem. Res. 2013, 52, 8856−8863

Table 3. The Influence of Storage over 46 Days on Surface Properties of PVTMS-Membrane Samples Modified by Low-Frequency Plasma

| discharge current, $I$, MA | time, $t$, sec | contact angle, $\theta$ [deg] | | adhesion work, $W_a$, mJ/m$^2$ | | surface energy, mJ/m$^2$ | | |
|---|---|---|---|---|---|---|---|---|
| | | water | glycerol | water | glycerol | $\gamma$ | $\gamma^d$ | $\gamma^p$ |
| | | 109 | 98 | 48.5 | 54.6 | 14.2 | 13.2 | 1.0 |
| 150 | 30 | 53 | 46 | 116.6 | 107.2 | 47.1 | 18.4 | 28.7 |
| 100 | 30 | 47 | 43 | 122 | 109.4 | 51.1 | 15.7 | 35.4 |
| 80 | 45 | 43 | 34 | 125.6 | 116.3 | 54.9 | 22.6 | 32.3 |
| 80 | 60 | 53 | 44 | 117.1 | 109 | 48 | 20.6 | 27.4 |
| 80 | 90 | 58 | 46 | 111.4 | 107.4 | 45.5 | 25.1 | 20.4 |

carboxyl-containing groups) and the absorption bands in the 3000−3600 cm$^{-1}$ range (which are characteristic of hydroxyl groups)[43] were examined. It was found that the glow discharge modification leads to the appearance of new absorption bands in the range from 3270 to 3400 cm$^{-1}$ and, at the same time, the intensity of the bands at 3400−3600 cm$^{-1}$ decreases. A shift of the specific OH-groups absorption bands to the low-frequency region can be associated with the development of a "network" of hydroxyl groups linked by hydrogen bonds on the modified PVTMS membrane surface. Plasmochemical modification triggers the formation of ketone groups with conjugated double bonds (1680−1690 cm$^{-1}$) and the absorption band corresponding to the double bond is shifted to lower frequencies (1660 cm$^{-1}$). Therefore, a specific "network" is formed on the surface of the plasma-modified PVTMS membrane due to the development of intermolecular hydrogen bonds.

**3.4. Formation of Charged States under Glow Discharge.** For the initial PVTMS membrane, the surface charge $Q$ is equal to −0.039 nC/cm$^2$. Figure 7 shows the

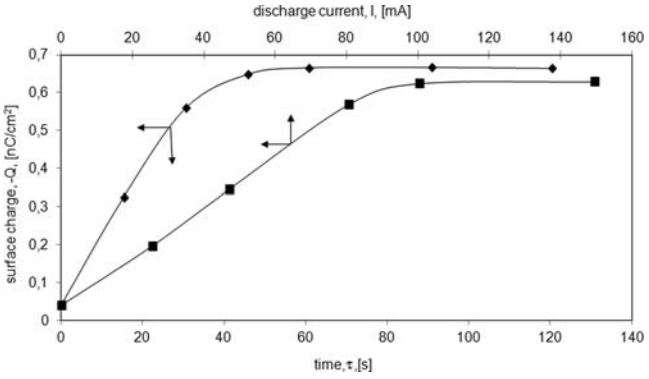


**Figure 7.** Surface charge plotted against the modification time at $I$ = 80 mA and discharge current at $\tau$ = 30 s.

surface charge ($Q$) plotted against the duration of low-frequency glow discharge treatment ($\tau$) in air (discharge current, 80 mA) and discharge current ($I$) (the treatment time, 30 s). As follows from Figure 7, in all cases, the $Q$ value is negative, and its absolute value increases with $\tau$ and $I$, and the plateau is attained at $\tau \geq 45$ s and $I \geq 80$ mA.

After storage in air at room temperature, the absolute $Q$ values decrease, but their sign remains invariable. Even within 10 days, the $Q$ value appears to be 7 times higher than that of the untreated sample.

For the initial membrane, the TSR and TSD currents (Figure 8) are nearly zero. After the plasma treatment, the PVTMS membrane surface became the negatively charged and the measured $Q$ value ($I$ = 80 mA, $\tau$ = 45 s) exceeded the initial potential by a factor of 16. Upon heating, the TSR currents

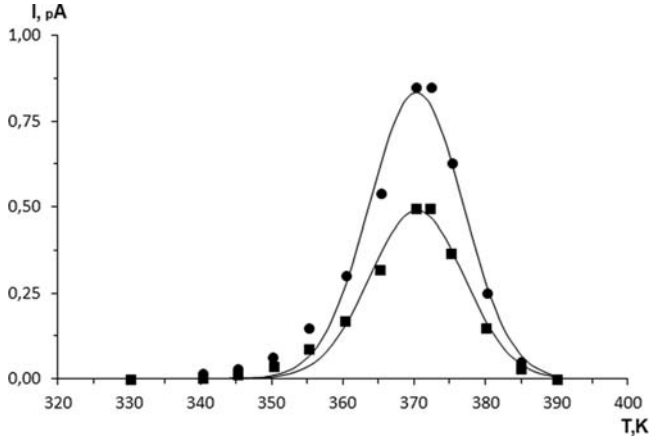


**Figure 8.** Thermograms of the TSP and TSD currents for the plasma-modified PVTMS membranes ($I$ = 80mA, time = 45 s.).

arise and their maximum is seen at 370 K; this maximum is associated with negative charge redistribution in the bulk of the sample (Figure 8); the activation energy of this process is $E$ = 0.75 ± 0.05 eV. Noteworthy is that this charge redistribution takes place near $T_g$ of the polymer. Moreover, according to ref 36, this relaxation process starts at ∼373 K. Polarization of the modified membrane in the external electric field at elevated temperatures entails a nonequilibrium charge redistribution, and the TSD curve passes its maximum in the same region as the TSR currents (Figure 8). Activation energy of the TSD process coincides with those of the TSR process. This indicates that, in these processes, the charge transfer proceeds via the common mechanism. The charge transfer in the membrane bulk can be explained in terms of the two following mechanisms: (1) movement of delocalized electrons via jumps over neighboring states[44] and (2) movement of ions that acquire mobility in the vicinity of the PVTMS main chain relaxation region.[36−38,45]

The entire body of the experimental data presented in Figure 9 in the $\theta$−$Q$ coordinates indicates that there exists a certain correlation between them. Similar dependence was observed in ref 35 for polyimide films after their low-frequency glow discharge modification. According to ref 39, formation of the charged states in the polymer surface layers markedly contributes to the improvement in hydrophilicity.

**3.5. Thermopervaporation Results.** For nitric acid solutions, we studied experimentally the TPV separation of volatile inorganic acids in the concentration range from 0.18 to 7.65 N at 343 K. The choice of this concentration interval is concerned with the practical problem in the separation of $HNO_3$ technological solutions for etching of metallic surfaces. The separation coefficient reads as


dx.doi.org/10.1021/ie3025246 | Ind. Eng. Chem. Res. 2013, 52, 8856−8863

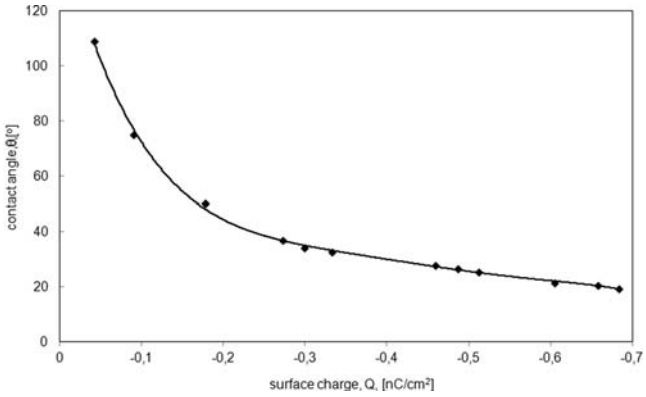


**Figure 9.** Contact angle plotted against surface charge for the plasma-modified PVTMS membranes.

$$\alpha = \frac{(x_j/x_i)_p}{(x_j/x_i)_j} \quad (3)$$

In Table 4, separation characteristics of the initial and modified PVTMS membranes with respect to the separation of nitric acid aqueous solutions are compared. Both initial and modified PVTMS membranes show water selective properties, namely, the permeate appears to be enriched with water. The total flux through the modified membrane is by 35−40% higher than that of the parent membrane, and both fluxes tend to decrease with increasing acid content in the feed solution. Examination of the contributions from partial water and acid fluxes to the total permeate flux through the membrane suggests that, in the studied concentration interval, the increase in the total permeate flux through the modified membranes can be explained by the related increase in the partial water flow. At the same time, in whole, the partial flux of nitric acid for the modified membrane is lower than that of the virgin membrane. This effect is observed for dilute solutions and it tends to decrease as the acid content in the feed solution increases. Hence, for low concentrations of nitric acid in the solution, the partial flux of nitric acid for the modified membrane decreases by more than an order of magnitude. When the content of acid in the feed solution increases, the partial acid flux for the initial and modified membranes tends to grow. The reduction in the total flux with increasing acid content in the feed solution is related to a decrease in the partial water flux whose contribution to the total flux dominates within this feed composition range. Most likely, this concentration dependence of the total and partial fluxes can be explained by changes in the driving force of the components' transport through the membrane and it correlates with the concentration dependence of the equilibrium pressure of the saturated vapors and the composition of vapor over aqueous solutions of nitric acid: the total vapor pressure and the content of water in the vapor decreases, whereas the content of the acid component in vapors increases with increasing concentration of nitric acid in the solution. This behavior of the partial fluxes manifests itself in the values of separation coefficients. As follows from Table 4, for the modified membranes, the $\alpha$ values are seen to increase. This effect is most pronounced for the TPV separation of the dilute nitric acid solutions. Moreover, for both modified and virgin membranes, their separation coefficient increases with increasing acid concentration in the feed solution. Hence, changes in surface characteristics of the PVTMS-based membranes from hydrophobic to hydrophilic entail an increase in the water flux and a rise in the separation selectivity. It is worth mentioning that the PVTMS membranes retain their mechanical and separation characteristics upon thermopervaporation experiments within the 6-month period.

This evidence suggests that both initial and modified PVTMS membranes appear to be stable to the action of inorganic acids over the entire concentration range and demonstrate high water-selective properties. The permeate flux for the modified membrane ranges, on average, from 1 to 2 kg/(m$^2$ h) at a feed temperature of 343 K and a temperature gradient across the membrane of 50 K. These characteristics fit the practical purposes of pervaporation separation. The temperature range suitable for the thermopervaporation separation of acid solutions corresponds to the range of the waste heat. As a result, this method seems to be very attractive for industrial applications.

**3.6. Comparison of the Separation Results.** Figure 10 presents the separation diagrams for MFF-2 and PVTMS initial and modified membranes as well as the liquid−vapor−equilibrium (LVE) curve of nitric acid aqueous solutions at 343 K. As follows from Figure 10, separation characteristics of the MFF-2 porous membranes roughly agree with the LVE

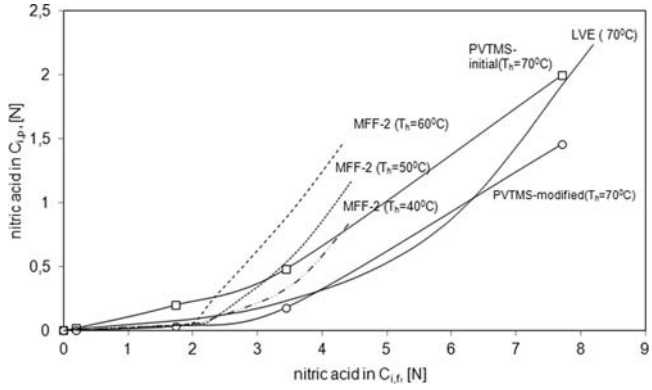


**Figure 10.** Separation diagrams for MFF-2, PVTMS-initial, and PVTMS-modified membranes for the separation of nitric acid aqueous solution.

**Table 4. Separation Characteristics of the Initial and Plasma Modified PVTMS Asymmetric Membranes with Respect to the Separation of Nitric Acid Aqueous Solutions ($T_h$ = 343 K, $T_c$ = 293 K)**

| PVTMS initial membrane | | | | | | PVTMS modified membrane | | | | | |
|---|---|---|---|---|---|---|---|---|---|---|---|
| $C_j$ in feed, N | $C_j$ in permeate, N | $J_t$ kg/m$^2$h | $J_j$, kg/m$^2$h | $J_i$, kg/m$^2$h | $\alpha$ | $C_i$ in permeate, N | $J_v$, kg/m$^2$h | $J_j$, kg/m$^2$h | $J_i$, kg/m$^2$h | $\alpha$ | $R_i$ |
| 0.18 | 0.018 | 1.28 | 1.2786 | 0,0014 | 10.3 | 0.0036 | 1.74 | 1,7439 | 0,0001 | 523 | 0.998 |
| 1.69 | 0.194 | 1.16 | 1.146 | 0,0139 | 9.3 | 0.0388 | 1.57 | 1,5667 | 0,0033 | 54 | 0.979 |
| 3.38 | 0.473 | 0.91 | 0,8738 | 0,0262 | 8.15 | 0.1690 | 1.28 | 1,2705 | 0,0135 | 23 | 0.946 |
| 7.65 | 1.989 | 0.68 | 0,600 | 0,079 | 5.06 | 1.4540 | 0.96 | 0,876 | 0,0836 | 7 | 0.783 |


dx.doi.org/10.1021/ie3025246 | Ind. Eng. Chem. Res. 2013, 52, 8856−8863

curve in the concentration interval from 0 to 2 N (concentration region I). As the nitric acid content in the feed increases (concentration region II), all curves for the MFF-2 membrane show a sharp break and the content of nitric acid in the permeate is higher than that expected from the LVE curve. This behavior can be explained by the fact that, above 2 N, the feed solution leakage through the membrane takes place. Therefore, certain amounts of the liquid feed solution can be nonselectively transported from the feed side to the liquid permeate. As compared with the LVE curve, nitric acid content in the permeate increases. Hence, concentration of nitric acid in the feed solution is equal to 2 N and this concentration can be considered as a certain wettability threshold for the MFF-2 membrane in the nitric acid aqueous solution. Noteworthy is that experiments on the separation of aqueous solutions of volatile acids in the concentration region I are well reproducible after the exposure of membranes in more concentrated feed solutions corresponding to the region II. Examination of the data presented in Table 1 suggests that the similar wettability threshold for the MFF-2/HCl system corresponds to 1 N hydrochloric acid content in the feed solution. The difference can be explained by the higher volatility of hydrochloric acid as compared with that of nitric acid. Hence, the acid component in the vapor phase may be involved in the possible mechanism of pore wetting. The wettability threshold should also affect the pickling solution separation by MD through the MFF-2 membrane. For nonvolatile components (for example, metal ions), the retention coefficients should markedly decrease when the content of the volatile acid is higher than the concentration value corresponding to the wettability threshold of the MFF-2 membrane for this acid.

For the nonporous asymmetric PVTMS membranes, the transport mechanism for the components, in general, obeys the solution-diffusion model. In contrast to the MFF-2 membrane, the curves for the initial and modified PVTMS membranes are seen to be smooth over the entire concentration range of the feed solutions (Figure 10). For the concentration region I, the separation characteristics of the PVTMS-modified membranes roughly agree with those of the MFF-2 membrane. Taking into account higher values of the total fluxes through the MFF-2 membrane, as compared with the modified PVTMS membrane (see Figure 4 and Table 4), one can conclude that, for this concentration interval, the MD process using the MFF-2 membrane seems to be advantageous over the TPV process using the modified PVTMS membrane. On the other hand, in the concentration region II, dewatering of nitric acid aqueous solutions appears to be more effective when the thermopervaporation through the modified PVTMS membrane, rather than the membrane distillation through the MFF-2 membrane, is used (see Figure 10).

## CONCLUSIONS

Conditions providing efficient treatment of the skin surface for the nonporous asymmetric PVTMS membranes in the low-frequency glow discharge are revealed. Plasma treatment is shown to improve the hydrophilicity of the membrane surface due to the chemical modification and formation of the negatively charged states.

Plasma treatment leads to the modification of the surface characteristics of the PVTMS membranes and to the improvement of both transport and selective characteristics of the initial asymmetric membranes in the TPV separation of inorganic acid aqueous solutions or, in other words, the total flux and separation coefficient toward water tend to increase.

The use of the porous hydrophobic MFF-2 membrane makes it possible to concentrate the dilute solutions of volatile inorganic acids by the MD method.

On the other hand, the use of nonporous PVTMS membranes allows water removal from the feed acid solutions. Hence, after the first stage of the pickling solution, separation through the porous MFF-2 membrane using the MD process, the resultant permeate can be concentrated at the second stage by the thermopervaporation through the plasma-modified PVTMS membrane.

## AUTHOR INFORMATION

### Corresponding Author

*Tel.: +7 495 9554293. E-mail: vvvolkov@ips.ac.ru.

### Notes

The authors declare no competing financial interest.

## ACKNOWLEDGMENTS

The authors gratefully acknowledge the support of the Ministry of Education and Science of the Russian Federation (GK No. 11.519.11.6003).

## ABBREVIATIONS

PVTMS = poly(vinyltrimethylsilane)
MD = membrane distillation
TPV = thermopervaporation
IR = infrared spectroscopy
TSR = thermostimulated relaxation
LVE = liquid−vapor−equilibrium
TSD = thermostimulated depolarization

### Nomenclature

$C$ = concentration (N)
$E$ = activation energy (eV)
$I$ = discharge current (mA)
$J$ = transmembrane flux (kg/(m$^2$ h))
$m$ = permeate mass (kg)
$Q$ = surface charge (nC/cm$^2$)
$S$ = membrane area (m$^2$)
$R$ = retention coefficient
$t$ = time of MD experiment (h)
$T$ = temperature, K
$V$ = flow rate (l/h)
$W_a$ = adhesion work (mJ/m$^2$)
$x$ = weight fraction

### Greek Letters

$\alpha$ = separation coefficient
$\varepsilon$ = dielectric permeability
$\gamma$ = surface energy (mJ/m$^2$)
$\theta$ = contact angle (°)
$\tau$ = plasma treatment time (s)
t = total

### Subscripts

c = cold
f = feed
i = inorganic acid
j = water
h = hot
p = permeate
t = total

### Superscripts

d = dispersion component
p = polar component

## REFERENCES


(1) Khayet, M. Membranes and theoretical modeling of membrane distillation: A review. *Adv. Colloid Interface Sci.* **2011**, *164*, 56.
(2) Lawson, W.; Lloyd, R. Membrane distillation. *J. Membr. Sci.* **1997**, *124*, 1.
(3) Lawson, K. W.; Lloyd, D. R. Membrane distillation. II. Direct contact MD. *J. Membr. Sci.* **1996**, *120*, 123.
(4) Phattaranawik, J.; Jiraratananon, R.; Fane, A. G. Effect of pore size distribution and air flux on mass transport in direct contact membrane distillation. *J. Membr. Sci.* **2003**, *215*, 75.
(5) Phattaranawik, J.; Jiraratananon, R.; Fane, A. G. Heat transport and membrane distillation coefficients in direct contact membrane distillation. *J. Membr. Sci.* **2003**, *212*, 177.
(6) Sarti, G. C.; Gostoli, C.; Matulli, S. Low energy cost desalination processes using hydrophobic membranes. *Desalination* **1985**, *56*, 227.
(7) Laganà, F.; Barbieri, G.; Drioli, E. Direct contact membrane distillation: modelling and concentration experiments. *J. Membr. Sci.* **2000**, *166*, 1.
(8) Li, B.; Sirkar, K. K. Novel membrane and device for direct contact membrane distillation-based desalination process. *Ind. Eng. Chem. Res.* **2004**, *43*, 5300.
(9) Song, L.; Li, B.; Sirkar, K. K.; Gilron, J. L. Direct contact membrane distillation-based desalination: Novel membranes, devices, larger-scale studies, and a model. *Ind. Eng. Chem. Res.* **2007**, *46*, 2307.
(10) Ugrozov, V. V.; Nikulin, V. N.; Elkina, I. B.; Zolotarev, P. P. Analytical method for calculating the process of contact membrane distillation in a flow-through membrane module. *Theor. Found. Chem. Eng.* **1995**, *29* (6), 535.
(11) Qtaishat, M.; Khayet, M.; Matsuura, T. Novel porous composite hydrophobic/hydrophilic polysulfone membranes for desalination by direct contact membrane distillation. *J. Membr. Sci.* **2009**, *341*, 139.
(12) Schofield, R. W.; Fane, A. G.; Fell, C. J. D. Gas and vapor transport through microporous membranes: I. Knudsen-Poisseuille transition. *J. Membr. Sci.* **1990**, *53*, 159.
(13) Schofield, R. W.; Fane, A. G.; Fell, C. J. D. Gas and vapor transport through microporous membranes: II. Membrane distillation. *J. Membr. Sci.* **1990**, *53*, 173.
(14) Fane, A. G.; Schofield, R. W.; Fell, C. J. D. The efficient use of energy in membrane distillation. *Desalination* **1987**, *64*, 231.
(15) Calabrò, V.; Jiao, B. L.; Drioli, E. Theoretical and experimental study on membrane distillation in the concentration of orange juice. *Ind. Eng. Chem. Res.* **1994**, *33*, 1803.
(16) Martinez-Diez, L.; Florido-Diaz, F. J. Desalination of brine by membrane distillation. *Desalination* **2001**, *137*, 267.
(17) Zolotarev, P. P.; Ugrozov, V. V.; Yolkina, I. B.; Nikulin, V. N. Treatment of waste water for removing heavy metals by membrane distillation. *J. Hazard. Mater.* **1994**, *37* (1), 77.
(18) Gostoli, C.; Sarti, G. C. Separation of liquid mixtures by membrane distillation. *J. Membr. Sci.* **1989**, *41*, 211.
(19) Sarti, G. C.; Gostoli, C.; Bandini, S. Extraction of organic components from aqueous streams by vacuum membrane distillation. *J. Membr. Sci.* **1993**, *80*, 21.
(20) Boi, C.; Bandini, S.; Sarti, G. C. Pollutants removal from wastewaters through membrane distillation. *Desalination* **2005**, *183*, 383.
(21) Drioli, E.; Wu, Y.; Calabro, V. Membrane distillation in the treatment of aqueous solutions. *J. Membr. Sci.* **1987**, *33*, 277.
(22) Tomaszewska, M.; Gryta, M.; Morawski, A. W. Study on concentration of acids by membrane distillation. *J. Membr. Sci.* **1995**, *102*, 113.
(23) Tomaszewska, M.; Mientka, A. Separation of HCl from HCl–$H_2SO_4$ solutions by membrane distillation. *Desalination* **2009**, *240*, 244.
(24) Thiruvenkatachari, R.; Manickam, M.; Kwon, T. O.; Moon, I. S.; Kim, J. W. Separation of water and nitric acid with porous hydrophobic membrane by air gap membrane distillation (AGMD). *Sep. Sci. Technol.* **2006**, *41*, 3187.
(25) Scott Sportsman, K.; DouglasWay, J.; Wen-Janq Chen, W-J.; Penz, P.; Laciak, V. The dehydration of nitric acid using pervaporation and a nafion perfluorosulfonate/perfluorocarboxylate bilayer membrane. *J. Membr. Sci.* **2002**, *203*, 155.
(26) Ames, L.; Douglas Way, J.; Bluhm, A. Dehydration of nitric acid using perfluoro-carboxylate ionomer membranes. *J. Membr. Sci.* **2005**, *249*, 65.
(27) Aptel, P.; Challard, N.; Cuny, J. Application of the pervaporation process to separate azeotropic mixtures. *J. Membr. Sci1.* **1976**, *1*, 271.
(28) Fernandez, E. S.; Geerdink, P.; Goetheer, E. L. V. Thermo pervap: The next step in energy efficient pervaporation. *Desalination* **2010**, *250*, 1053.
(29) Borisov, I. L.; Volkov, V. V.; Kirsh, V. A.; Roldugin, V. I. Simulation of the temperature-driven pervaporation of dilute 1-butanol aqueous mixtures through a PTMSP membrane in a cross-flow module. *Pet. Chem.* **2011**, *51*, 542.
(30) Volkov, V. V.; Borisov, I. L. Thermopervaporation membrane bioreactor as a new concept for the low-cost production of biobutanol. *Proc. Eng.* **2012**, *44*, 278.
(31) Yampolskii, Yu. P; Volkov, V. V. Studies in gas permeability and membrane gas separation in the Soviet Union. *J. Membr. Sci.* **1991**, *64*, 191.
(32) Gilman, A. B.; Shifrina, R. R.; Potapov, V. K.; Tuzov, L. S.; Vengerskaya, L. E.; Ggrigor'eva, G. A. The alternation of properties and structure of polyimide surface under glow discharge. *High Energy Chem.* **1993**, *27*, 79.
(33) Wu, S. *Polymer Interfaces and Adhesion*; Marcel Dekker: New York, 1982.
(34) Sessler, G. M. *Electrets*; Springer-Verlag: Berlin-Heidelberg-New York, 1980.
(35) Gilman, A. B.; Drachev, A. I.; Kuznetsov, A. A.; Potapov, V. K. Modification of polyimide films of different thickness in direct-current discharge. *High Energy Chem.* **1998**, *32*, 483.
(36) Volkov, V. V.; Novitskii, E. G.; Durgaryan, S. G.; Nametkin, N. S. The study of the transitions and relaxation phenomena in poly(vinyltrimethyl silane) by means of IR spectroscopy. *Dokl. Akad. Nauk SSSR* **1978**, *238*, 600.
(37) Antipov, E. M.; Polikarpov, V. M.; Semenov, O. B.; Khotimsky, V. S.; Plate, N. A. On the mesophase state of poly-(vinyltrimethylsilane). *Vysokomol. Soedin.* **1990**, *32*, 2404.
(38) Antipov, E. A.; Polikarpov, V. M.; Volkov, V. V.; Frenkin, E. I. Structure of mesophase poly(vmyltrimethyl silane). *Vysokomol. Soedin.* **1991**, *33*, 2135.
(39) Gilman, A. B.; Drachev, A. I.; Kuznetsov, A. A.; Pavlov, S. A.; Potapov, V. K. Effect of charge states on wettability of polyimide films modified in a low-frequency glow-discharge plasma. *High Energy Chem.* **1996**, *30*, 373.
(40) Smolders, K.; Franken, A. C. M. Terminology for membrane distillation. *J. Membr. Sci.* **1989**, *72*, 249.
(41) Reid, R. C.; Prausnitz, J. M.; Poling, B. E. *The Properties of Gases and Liquids*; McCraw-Hill: New York, 1987
(42) Tomaszewska, M.; Gryta, M.; Morawski, A. W. The influence of salt in solution on hydrochloric acid recovery by membrane distillation. *Sep. Purif. Technol.* **1998**, *14*, 183.
(43) Lin-Vien, D.; Colthup, N. B.; Fately, W. G.; Grasseli, J. G. *The Handbook of Infrared and Raman Characteristic Frequencies of Organic Molecules*; Academic Press: New York, 1991.
(44) Mott N.; Davis, E. *Electron Processes in Noncrystalline Materials*; Clarendon Press: Oxford, 1979.
(45) Volkov, V. V.; Novitskii, E. G.; Durgaryan, S. G.; Nametkin, N. S. The study of the transitions and relaxation phenomena in poly(vinyltrimethyl silane) by means of IR spectroscopy. *Dokl. Akad. Nauk SSSR* **1978**, *238*, 600.